Proceedings Paper:
Ball, E. orcid.org/0000-0002-6283-5949 and Joseph, S.D. (2023) Design and measurement of a GaAs MMIC for use in a 73 GHz time modulated array. In: 2023 IEEE Conference on Antenna Measurements and Applications (CAMA) Proceedings. 2023 IEEE Conference on Antenna Measurements and Applications (CAMA), 15-17 Nov 2023, Genoa, Italy. Institute of Electrical and Electronics Engineers (IEEE) , pp. 560-563. ISBN 9798350323054

https://doi.org/10.1109/CAMA57522.2023.10352864

Design and Measurement of a GaAs MMIC for use in a 73 GHz Time Modulated Array

Edward A. Ball, Sumin David Joseph
Department of Electroninc & Electrical Engineering
The University of Sheffield
Sheffield, United Kingdom
{e.a.ball, s.d.joseph}@sheffield.ac.uk

***Abstract*— A GaAs MMIC using 0.1 µm pHEMTS is designed to realize a gain & phase switching module for use in a Time-Modulated Array (TMA) for transmit or receive at 73 GHz. As part of the MMIC design, a novel technique to implement phase inversion switching is introduced- maintaining good input and output RF match regardless of phase switch state. Lab measured results for 16 dies are presented. At 73 GHz the tested MMICs have an average gain within 1.1 dB of simulation and phase inversion switching within 3 degrees of a 180 degree requirement.**

***Keywords*— time-modulated arrays (TMA), millimeter wave circuits, MMIC.**

I. INTRODUCTION

A possible alternative and underused yet novel strategy for a phased array is to use time-modulated array switching to implement an effective phase shift at each radiating element and hence create a Time Modulated Array (TMA) [1]-[5]. The TMA avoids the need for analog phase shifters and requires only simple digital control interfaces.

One problem with the TMA concept has been the removal of the boresight beam, which cannot be steered. This was addressed in [6] by use of a time averaging strategy with a three-state amplifier, rather than the traditional TMA on / off RF switching function. From [6] it is apparent that the TMA switch performance is critical to the performance of the TMA. The switching circuit cell identified in [6] is required to change the gain states quickly over a 10 dB range and must also quickly switch between 0 and 180 degrees of phase, depending on the required beam steering angle.

To test the feasibility of the TMA at mmWave frequencies for future mobile applications, a dedicated hardware platform is introduced, centered on 73 GHz in the E band spectrum allocation. Due to the lack of off-the-shelf RF mmWave hardware, a bespoke GaAs MMIC has been designed and manufactured to implement the TMA switching cell and is the focus of this paper, with laboratory results reported for sixteen devices.

II. TMA SYSTEM OVERVIEW

A TX system of eight TMA controller cell MMICs and 73 GHz series fed arrays (SFA) [7], [8] as radiating structures is shown in Fig. 1. The use of the SFA sub-arrays form a pencil beam that can be steered by the TMA. Although 1D steering is discussed in our work, it is conceptually possible to create a 2D array using a TMA by employing a 2D matrix of patch antennas or similar.

The array factor (AF) of an N radiating element TMA using an element-specific switch on duration T_k, turn on delay T_{0k} and with frame period Tp can be expressed by (1) [6].

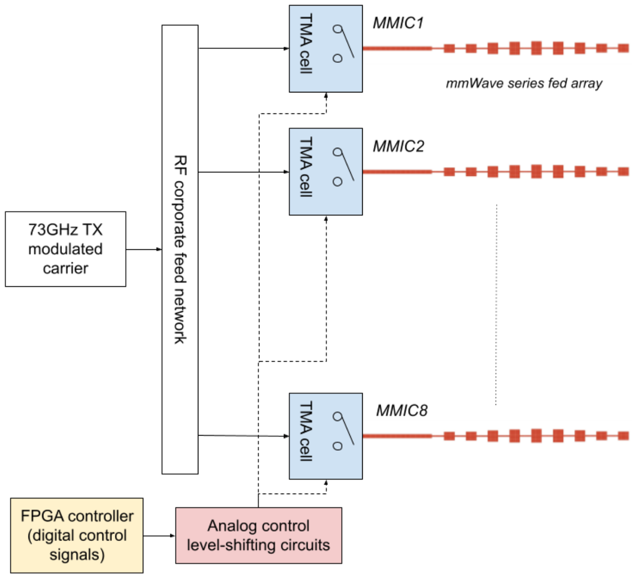

Fig. 1. Conceptual eight element 73 GHz TMA TX array using MMICs and SFAs.

$$AF(\theta, n, t) = e^{j[\omega_c + n.\omega_p]t} . \sum_{k=1}^{N} e^{j\varphi_k} . \frac{\sin\left(n\pi \frac{T_k}{T_p}\right)}{n\pi} . e^{-jn\pi\left(2\frac{T_{0k}}{T_p} + \frac{T_k}{T_p}\right)} \quad (1)$$

The time modulation of the RF signal at element k can be represented as a series of Fourier coefficients, multiplied with harmonic n of the switching frequency ω_p, which are then up converted to the carrier frequency ω_c. In the TX case, this produces a steered beam at ($\omega_c + n\ \omega_p$). The term $e^{j\varphi_k}$ in (1) is an element-specific phase shift, which is a function of radiating element spacing and evaluated beam angle. It can be expressed using (2), where d is the spacing between the elements, θ is the azimuth beam angle direction being evaluated and λ is the carrier wavelength.

$$\varphi_k = (k-1)\frac{2\pi}{\lambda} d \sin(\theta) \quad (2)$$

The control signals for the array are simple digital logic signals (shifted in level to suit the MMICs), with their relative timings defining the array steering. The digital control selects the required TMA cell gain (from two fixed settings) and required phase (0 or 180 degrees) [6].

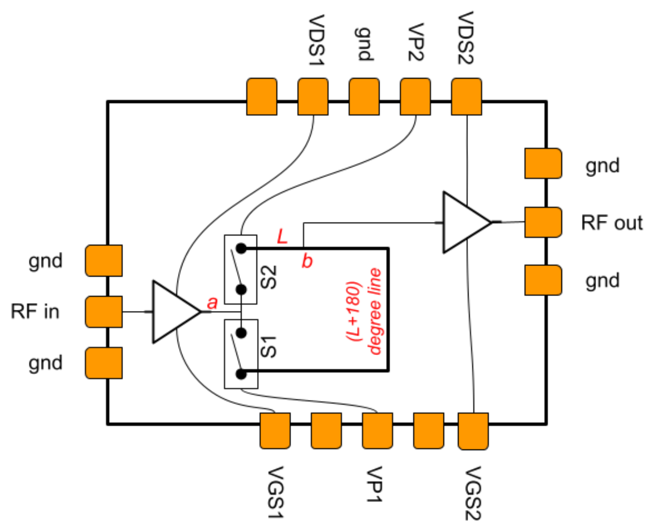

Fig. 2. 73 GHz MMIC architecture for one TMA cell.

III. MMIC Design

To implement the required TMA cell switching function for use in Fig. 1, based on [6], requires both fast changing gain states and 0 or 180 degree phase states in each MMIC. The simplified MMIC chip concept is shown in Fig. 2. The MMIC can serve as either a TX TMA cell, or by reversing the chip orientation in the array, as an RX TMA cell. The MMIC is manufactured using the UMS PH10 pHEMT process, with foundry design kits imported into Keysight ADS.

A novel feature of our design is the 0 or 180 degree phase switcher. This uses two ‘cold’ pHEMTs (complementary switches S1 and S2 in Fig. 2) with RF inputs connected together at point *a,* and through a 180-degree line connecting the outputs together at point *b*. Since one or other of the pHEMT switches is always *on* and the other always *off* (depending on the desired 0 or 180 degrees of signal phase) and MMIC transistors are expected to be very similar, the impedances presented at the combined switch input (point *a*) and the combined output (point *b*) should not change significantly. Note that point *b* will always see an off-state impedance from one switch and an on-state impedance from the other switch and the 180-degree line has no impedance-transforming effect. The resulting constant input and output impedances of the switching subcircuit thus allows for a simple 50 ohm matching circuit design and easier interface to the adjacent input and output amplifier stages. The MMIC system phase is controlled by applying complementary voltages of ±0.8 V to *VP1* (for S1) and ∓0.8 V to *VP2* (for S2). We define Phase State 1 as when *VP1* is positive, and Phase State 2 as when *VP1* is negative.

Both the input and output amplifier stages are single device (2 x 20 µm gates) common source pHEMTs, biased at 0 V *Vgs* for a maximum gain setting. *Vgs1* is then reduced to a lower voltage to implement the required -10 dB relative gain reduction control. The input and output stage amplifying pHEMTs are biased at 3 V *Vds* and are each stabilized at 20 GHz and 40 GHz using a series 650 ohms resistor and 0.5 pF capacitor between drain and gate.

Incorporation of the wire bond links into the RF matching to the die must be considered at mmWave frequencies. In some approaches, a low pass filter (LPF) strategy incorporating the bond wire is used [9]. However, in our work the GSG pads of the die are included in the design and matched out to 50 ohms on the die using transmission line stubs. Subsequent bond wire effects are then matched out on the full TMA PCB.

IV. MMIC Lab Tests

All MMIC dies were tested at [10] using a Keysight PNA N5245B with WR15+ VDI frequency extenders and Picoprobe 120-GSG-150-BT RF wafer probes, calibrated using an AC2-2 wafer. The DC signals are provided using dedicated DC probe cards from MPI. A micrograph of one of the MMICs undergoing tests is shown in Fig. 3.

The die measured RF data for sixteen MMICs is compared to Keysight ADS simulations in Fig. 4 to Fig. 7. At 73 GHz the MMIC gain is within 1.5 dB of simulation. It is also important that the gains for each phase state are similar at 73 GHz and this is seen, though with the best alignment at 72 GHz (as also seen in simulation). The *VP1* and *VP2* controlled phase state gain difference is better than 2 dB between 69 GHz and 76 GHz. The required 180-degree phase shift control is also achieved, between the phase states.

From Fig. 6 and Fig. 7 the input and output return losses are not a strong function of the phase switching state. This confirms the impedances provided by the phase inverter subcircuit at points *a* and *b* (Fig. 2) are not varying significantly and confirms good operation of this circuit. Though the input return loss null of S11 is shifted from the simulation it is acceptable, and the output return loss S22 is good.

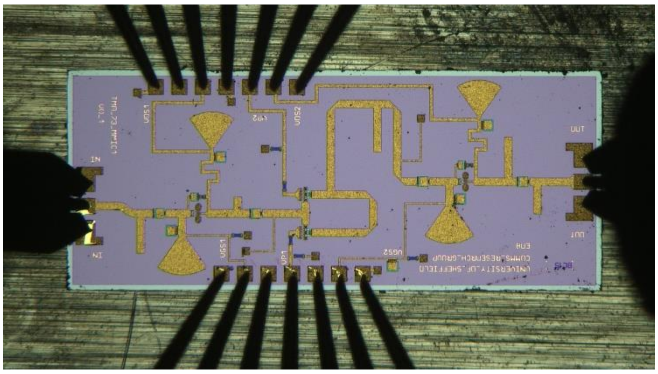

Fig. 3. Micrograph of die (1.4mm x 3.4mm) with RF and DC probes attached.

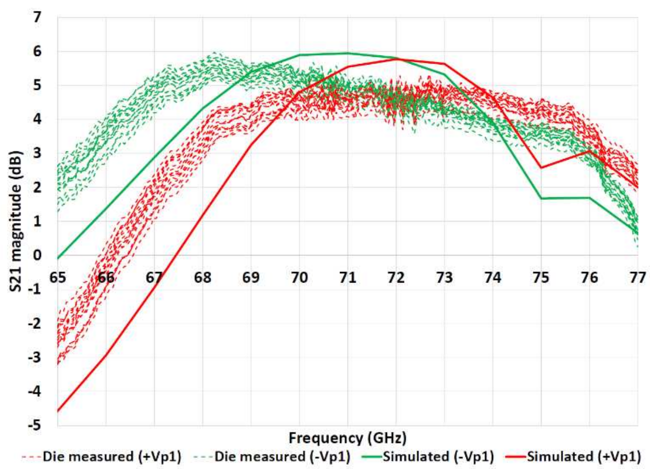

Fig. 4. Measured & simulated S21 gain for both phase states (*Vgs1* = 0 V).

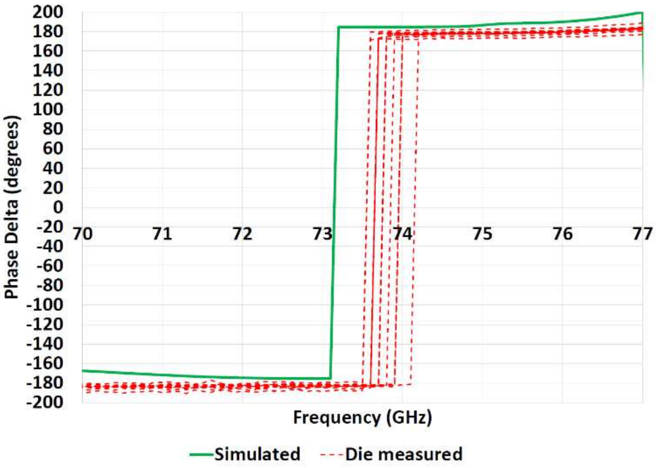

Fig. 5. Measured & simulated output phase delta control (due to *VP1* & *VP2* control), *Vgs1* = 0 V. Desired 180 degree phase control is seen.

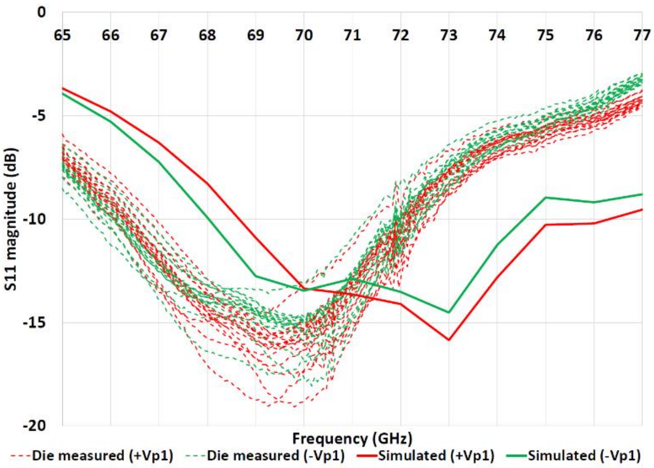

Fig. 6. Measured & simulated S11 for both phase states (*Vgs1* = 0 V).

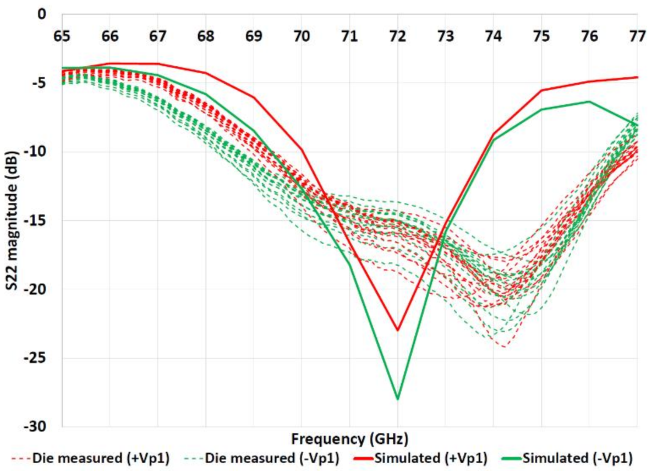

Fig. 7. Measured & simulated S22 for both phase states (*Vgs1* = 0 V).

The key performance criteria at 73 GHz for the sixteen bare MMICs are compared to circuit simulation expectations in Table 1. From Keysight ADS EM circuit co-simulations, the 180-degree phase change can be fully executed and settled within 400 ps and the gain change is settled within 200 ps.

TABLE I. MMIC RESULTS COMPARISON AT 73 GHZ.

Parameter	Simulation	Measurement (Average across 16 dies)	
Gain (Phase State 1 / Phase State 2)	5.6 / 5.3	4.7 / 4.2	dB
Gain control range	10 (*Vgs1*: 0 V to -0.45 V)	10 (*Vgs1*: 0 V to -0.5 V)	dB
10 dB gain change control delay	184	-	ps
Phase change shift	175	183	degrees
Phase change control delay	391	-	ps
Total DC current (*Vgs1 = 0V, Vgs2 = 0V*)	15.0	20.4	mA
Input return loss	15	8	dB
Output return loss	15	18	dB
P1dBO / Psat	2.8 / 9.8	-	dBm

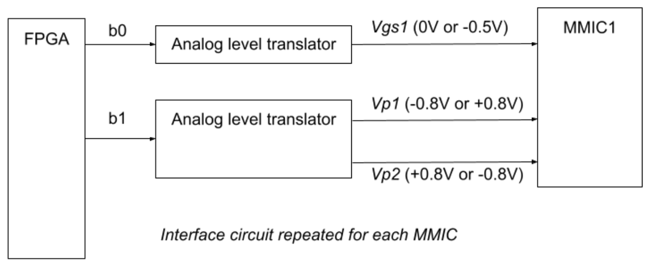

Fig. 8. FPGA to MMIC interface (for 1 cell).

In the TMA, each MMIC will be interfaced to an FPGA for binary control via two digital lines and simple analog level shifters, as shown conceptually in Fig. 8. Hence in total, only sixteen digital lines are needed to control the eight MMICs and thus control the array beam steering.

It should be noted that unlike other digitally controlled phase shifters, where the number of digital lines *M* defines the phase step size (due to 2^M steps across a maximum phase range), the TMA only needs to control each MMIC using two digital lines. The two lines select between the two required gain states controlled using *Vgs1*, and the complimentary phase inverter states controlled by *VP1* and *VP2*. In the array, the actual carrier phase and hence beam steer created is due to the action of the Fourier series generated by the effective RF switching timings from (1). Therefore, the achieved carrier phase step size is limited only by the FPGA time step precision, not the MMIC or number of control lines. In contrast, in conventional analog controlled phase shifter chips, the phase resolution would depend on the resolution of the applied control voltage, from a DAC or similar. A comparison of the MMIC when in the TMA with respect to other conventional phase shifter chips is made in Table 2, showing the TMA competitiveness.

CONCLUSION

This paper presents the TMA concept and test results for sixteen GaAs MMICs operating at 73 GHz. The MMIC is designed to support a TX or RX TMA research test platform. The tested MMIC performance agrees well with circuit simulation expectations and has good gain balance between two fixed phase states and sufficient phase change switching.

TABLE II. COMPARISON OF MMIC IN TMA TO OTHER MMWAVE PHASE SHIFTER ARCHITECTURES.

Ref.	Carrier / BW (GHz)	Technology	Die area (mm^2)	DC power (mW)	Gain (dB)	Switching speed	Control
[11]	39.5 / 5	GaAs pHEMT	2.4	63	-12.8	n/a	Digital (3 bits)
[12]	38 / 3	GaAs pHEMT	0.87	0	-10.7	n/a	Digital (4 bits)
[13]	11 / 13	GaAs	3.7	0	-8	20 ns	Analogue (0-10V)
This work	73 / 7	GaAs pHEMT	4.8	61.2	+4.7	391 ps	digital (2 bits)

Overall, the MMIC has proved suitable for use in the TMA platform.

The reported circuit technique for implementing fast switching phase inversion, with non-varying terminating impedance, could be useful in other applications.

ACKNOWLEDGMENT

This work was supported by the U.K. Research and Innovation (UKRI) Future Leaders Fellowship under Grant MR/T043164/1.

REFERENCES

[1] W. H. Kummer, A. T. Villeneuve, T. S. Fong, and F. G. Terrio, "Ultra-low sidelobes from time-modulated arrays," *IEEE Trans. Antennas Propag*., vol. 11, no. 6, pp. 633–639, 1963

[2] P. Rocca, G. Oliveri, R. J. Mailloux, and A. Massa, "Unconventional phased array architectures and design methodologies - a review," *Proceedings of the IEEE*, vol. 104, no. 3, pp. 544–560, Mar. 2016. doi: 10.1109/JPROC.2015.2512389.

[3] G. Li, S. Yang, Y. Chen, and Z. Nie, "A novel beam scanning technique in time modulated linear arrays," in IEEE Antennas and Propagation Society, AP-S International Symposium (Digest), 2009. doi: 10.1109/APS.2009.5171609.

[4] W. Q. Wang, H. C. So, and A. Farina, "An overview on time/frequency modulated array processing," IEEE Journal on Selected Topics in Signal Processing, vol. 11, no. 2, pp. 228–246, Mar. 2017, doi: 10.1109/JSTSP.2016.2627182.

[5] Y. Tong and A. Tennant, "Simultaneous control of sidelobe level and harmonic beam steering in time-modulated linear arrays," Electron Lett., vol. 46, no. 3, pp. 200–202, 2010, doi: 10.1049/el.2010.2629.

[6] E. A. Ball and A. Tennant, "A technique to control the harmonic levels in time-modulated antenna arrays - theoretical concept and hardware verification platform," IEEE Trans. Antennas Propag., vol. 68, no. 7, pp. 5375–5386, Jul. 2020, doi: 10.1109/TAP.2020.2978894.

[7] E. A. Ball, "Investigation into series-fed microstrip patch arrays at 26 GHz, 28 GHz and 48 GHz - design, simulation and prototype tests," in Proceedings of the 2021 IEEE Texas Symposium on Wireless and Microwave Circuits and Systems: Making Waves in Texas, WMCS 2021, May 2021. doi: 10.1109/WMCS52222.2021.9493271.

[8] B. Jian, J. Yuan, and Q. Liu, "Procedure to design a series-fed microstrip patch antenna array for 77 GHz automotive radar," in 2019 Cross Strait Quad-Regional Radio Science and Wireless Technology Conference (CSQRWC), Jul. 2019, pp. 1–2. doi: 10.1109/CSQRWC.2019.8799356.

[9] T. P. Budka, "Wide-bandwidth millimeter-wave bond-wire interconnects," IEEE Trans. Microw. Theory Tech., vol. 49, no. 4 I, pp. 715–718, Apr. 2001, doi: 10.1109/22.915447.

[10] The National mmWave Measurement Laboratory. [Online]. Available: https://mmwave.group.shef.ac.uk/.

[11] Z. Qiu, J. Liu, H. Xu, G. Su, and L. Sun, "A 37-42 GHz Continuous Tunable Phase Shifter in 150 nm GaAs pHEMT," in 2019 12th UK-Europe-China Workshop on Millimeter Waves and Terahertz Technologies (UCMMT), 2019, pp. 1–3. doi: 10.1109/UCMMT47867.2019.9008321.

[12] M. S. Yang, Y. T. Lin, K. Y. Kao, and K. Y. Lin, "A compact E-mode GaAs pHEMT phase shifter MMIC for 5G phased-array systems," in Asia-Pacific Microwave Conference Proceedings, APMC, Dec. 2019, pp. 488–490. doi: 10.1109/APMC46564.2019.9038465.

[13] "HMC247 data sheet," Analog Devices Ltd.